Distinct regulations driving YAP1 expression loss in poroma, porocarcinoma and RB1 -deficient skin carcinoma

Thibault Kervarrec, Eric Frouin, Christine Collin, Anne Tallet, Matthias Tallegas, Daniel Pissaloux, Franck Tirode, Serge Guyétant, Mahtab Samimi, Pauline Gaboriaud, et al.

HAL Id: hal-04077169
https://hal.inrae.fr/hal-04077169

Submitted on 21 Apr 2023

Histopathology

Distinct regulations driving YAP1 expression loss in poroma, porocarcinoma and *RB1*-deficient skin carcinoma

Thibault Kervarrec,[1,2,3] (iD) Eric Frouin,[1,4] Christine Collin,[5] Anne Tallet,[5] Matthias Tallegas,[5] Daniel Pissaloux,[6,7] (iD) Franck Tirode,[6,7] Serge Guyétant,[2,3,4] Mahtab Samimi,[8] Pauline Gaboriaud,[3] Antoine Touzé,[3] David Schrama,[9] Roland Houben,[9] Flore Tabareau-Delalande,[10] Anne Neuhart,[6] Arnaud de la Fouchardière,[1,6,7] Amélie Osio,[1,11,12] Bénédicte Cavelier–Balloy,[13] Sara Laurent-Roussel,[12,13] Pierre Sohier,[1,14,15] Tilmant Cyprien,[1,16] Brigitte Balme,[1,17] Fanny Belzung,[18] Marie-Laure Jullie,[1,18] Bernard Cribier,[1,19] Maxime Battistella[1,11] & Nicolas Macagno[1,20,21]

[1]CARADERM, French Network of Rare Cutaneous Cancer, Lille, [2]Department of Pathology, University Hospital of Tours, [3]'Biologie des Infections à Polyomavirus' Team, UMR1282 INRAE, University of Tours, Tours, [4]Department of Pathology, University Hospital of Poitiers, University of Poitiers, LITEC, Poitiers, [5]Platform of Solid Tumor Molecular Genetics, University Hospital Center of Tours, Tours, [6]Department of Biopathology, Center Léon Bérard, [7]University of Lyon, Université Claude Bernard Lyon 1, INSERM 1052, CNRS 5286, Centre Léon Bérard, Cancer Research Center of Lyon, Equipe Labellisée Ligue contre le Cancer, Lyon, [8]Department of Dermatology, University Hospital Center of Tours, Tours, France, [9]Department of Dermatology, Venereology and Allergology, University Hospital Würzburg, Würzburg, Germany, [10]Department of Pathology, Hospital Centrer of Orléans, Orléans, [11]Department of Pathology, Hospital Saint-Louis, AP-HP, Université Paris Cité, INSERM U976, Paris, [12]Centre National de Dermatopathologie, Paris-la Roquette, Ivry, [13]Cabinet Mathurin Moreau, [14]Department of Pathology, Hôpital Cochin, AP-HP, AP-HP.Centre – Université Paris Cité, [15]Faculté de Médecine, University Paris Cité, Paris, [16]Department of Pathology, Groupement des Hopitaux de l'institut catholique de Lille, Lille, [17]Department of Pathology, University Hospital of Lyon Sud, Lyon, [18]Department of Pathology, University Hospital of Bordeaux, Bordeaux, [19]Clinique Dermatologique, Hôpitaux Universitaires et Université de Strasbourg, Hôpital Civil, Strasbourg, [20]Department of Pathology, APHM, Timone University Hospital and [21]Aix-Marseille University, INSERM U1251, MMG, Marseille, France

---

Kervarrec T, Frouin E, Collin C, Tallet A, Tallegas M, Pissaloux D, Tirode F, Guyétant S, Samimi M, Gaboriaud P, Touzé A, Schrama D, Houben R, Tabareau-Delalande F, Neuhart A, de la Fouchardière A, Osio A, Cavelier–Balloy B, Laurent-Roussel S, Sohier P, Cyprien T, Balme B, Belzung F, Jullie M-L, Cribier B, Battistella M & Macagno N

(2023) *Histopathology* **82**, 885–898. https://doi.org/10.1111/his.14874

Distinct regulations driving YAP1 expression loss in poroma, porocarcinoma and *RB1*-deficient skin carcinoma

Aims: Recently, *YAP1* fusion genes have been demonstrated in eccrine poroma and porocarcinoma, and the diagnostic use of YAP1 immunohistochemistry has been highlighted in this setting. In other organs, loss of *YAP1* expression can reflect *YAP1* rearrangement or transcriptional repression, notably through *RB1* inactivation. In this context, our objective was to re-evaluate the performance of YAP1 immunohistochemistry for the diagnosis of poroma and porocarcinoma.

Methods and results: The expression of the C-terminal part of the YAP1 protein was evaluated by

Address for correspondence: Thibault Kervarrec, Department of Pathology, Hôpital Trousseau, CHRU de Tours, 37044 TOURS Cedex 09, France. e-mail: thibaultkervarrec@yahoo.fr
Thibault Kervarrec and Eric Frouin equally contributed to the present study

immunohistochemistry in 543 cutaneous epithelial tumours, including 27 poromas, 14 porocarcinomas and 502 other cutaneous tumours. Tumours that showed a lack of expression of YAP1 were further investigated for Rb by immunohistochemistry and for fusion transcripts by real-time PCR (*YAP1*::*MAML2* and *YAP1*::*NUTM1*). The absence of YAP1 expression was observed in 24 cases of poroma (89%), 10 porocarcinoma (72%), 162 Merkel cell carcinoma (98%), 14 squamous cell carcinoma (SCC) (15%), one trichoblastoma and one sebaceoma. Fusions of *YAP1* were detected in only 16 cases of poroma ($n = 66\%$), 10 porocarcinoma (71%) all lacking YAP1 expression, and in one sebaceoma. The loss of Rb expression was detected in all cases except one of YAP1-deficient SCC ($n = 14$), such tumours showing significant morphological overlap with porocarcinoma. *In-vitro* experiments in HaCat cells showed that *RB1* knockdown resulted in repression of YAP1 protein expression.

Conclusion: In addition to gene fusion, we report that transcriptional repression of *YAP1* can be observed in skin tumours with *RB1* inactivation, including MCC and a subset of SCC.

Introduction

Eccrine poroma is a benign adnexal tumour with differentiation towards the intradermal portion of the sweat glands apparatus.[1] Histologically, poroma is composed of a mixture of poroid and cuticular cells. Depending on its silhouette and location, four poroma subtypes have been described: *hidracanthoma simplex* (intraepidermal poroma), poroma, poroid hidradenoma (dermal nodular poroma) and dermal duct tumour.[1]

Porocarcinoma represents the malignant counterpart of poroma, with a 5-year estimated overall survival rate of 69%.[2] Porocarcinoma occurs preferentially on the lower limb in elderly patients.[3,4] Histologically, 20% of porocarcinoma cases are associated with a benign poroma component, suggesting the possibility of a progression from a benign precursor.[3]

The distinction between porocarcinoma and poorly differentiated squamous cell carcinoma (SCC) on morphological and immunohistochemical grounds can be challenging in current practice and based on reported criteria.[3,5] Although immunohistochemical detection of carcinoembryonic antigen (CEA) and epithelial membrane antigen (EMA) to highlight the ductal structures support the diagnosis of porocarcinoma, their diagnostic performance has not been evaluated for molecularly confirmed cases.[3,6]

In 2019, Sekine *et al.* reported in eccrine poroma and porocarcinoma the detection of recurrent rearrangements of *YAP1*, a gene encoding for a downstream effector of the Hippo pathway, either with *MAML2* or *NUTM1*.[7] Furthermore, the authors demonstrated that fusion of *YAP1* resulted in the loss of expression of the C-terminal part of the YAP1 protein (C-ter YAP1), a phenomenon that can be detected by immunohistochemistry. The authors demonstrated the absence of C-ter YAP1 expression in 96.2% of the poromas ($n = 100$) and 63.6% of the porocarcinomas ($n = 7$), while YAP1 expression was preserved in a cohort of cutaneous control tumours ($n = 87$), suggesting that it could serve as a surrogate to molecular biology. More recently, Russell-Goldman *et al.* confirmed such findings by demonstrating the lack of C-ter YAP1 expression in seven of 12 porocarcinomas (58%) and eight of 10 poroma (80%) while it was always preserved in controls.[8] In parallel, nuclear protein in testis (NUT) immunohistochemistry has been highlighted to screen *NUTM1*-rearrangement in poroid hidradenoma.[17]

In line with these findings, the loss of C-ter YAP1 expression in the skin has been demonstrated in mesenchymal neoplasms with rearrangement of the *YAP1*, i.e. epithelioid haemangioendothelioma harbouring *YAP1*::*TFE3* fusion transcript.[9] Moreover, it has also been observed in neuroendocrine cancers of the lung and prostate,[10,11] these findings being not related to *YAP1* gene rearrangement but due to *YAP1* transcriptional repression mediated by *RB1* inactivation.[11] Importantly, in the skin, *RB1* inactivation is a main determinant of the development of Merkel cell carcinoma (MCC), a rare skin cancer mainly induced by Merkel cell polyomavirus (MCPyV) integration,[12] and was further reported in SCC[13] and adnexal tumours, including sebaceous carcinoma[14] and porocarcinoma.[15]

In this context, the goal of the present study was (1) to re-evaluate the performances of C-ter YAP1 immunohistochemical detection for poroma and porocarcinoma diagnosis and (2) to determine whether the absence of C-ter YAP1 expression constantly reflects the presence of the fusion protein or might otherwise be caused by transcriptional down-regulation in skin tumours.

Methods

DESIGN AND SETTINGS

The cohort consisted of various subtypes of cutaneous tumours embedded in tissue microarray (TMA, $n = 511$) and studied on whole-slides ($n = 32$), which were extracted from the archives of four pathology departments[3] (Tours, Marseille, Bordeaux and Poitiers, France), and from a historical/prospective multicentric French cohort of patients with a diagnosis of MCC established between 1998 and 2020.[16] All cases were reviewed collegially by at least two pathologists to confirm diagnosis before inclusion (M.B., B.C., N.M., E.F., S.G., T.K.) (Local Ethics Committee in Human Research, Tours, France; no. ID RCB 2009-A01056-51). Due to the TMA approach, only cases with at least one representative spot were included in the present study.

IMMUNOHISTOCHEMISTRY

YAP1 expression was evaluated by immunohistochemistry in all cases. For TMA inclusion, the selected areas were extracted by using a 1-mm tissue core and cores were mounted in triplicate on the tissue microarray by using a semi-motorised tissue array system (MTA booster OI version 2.00, Alphelys). Expression of all investigated markers was assessed using a BenchMark ULTRA Platform, as instructed by the manufacturer. Antibodies and dilutions are displayed in Supporting information, Method S1.

The immunohistochemical staining was evaluated independently by at least two pathologists (N.M., E.F., T.K.) who were blinded to the clinical and molecular data. Discordant cases were subsequently reviewed collegially, and ambiguous cases were reviewed on whole-slide examination. The interpretation of immunohistochemistry (staining categories) was predetermined as previously described.[7,15,17] The expression of YAP1 and Rb were classified as preserved, heterogeneous (partial loss) or lost. The nuclear expression of NUT was evaluated in cases with *YAP1::NUTM1* fusion and classified as present or absent. The expression of Rb was evaluated on whole-slides in porocarcinoma cases and in some of the SCC cases considered as 'porocarcinoma mimickers' ($n = 32$).

DETECTION OF FUSION TRANSCRIPTS BY POLYMERASE CHAIN REACTION (PCR)

The presence of *YAP1::MAML2* and *YAP1::NUTM1* fusion transcripts was investigated in all *YAP1*-deficient tumours and 10 cases of MCC using reverse transcription-quantitative polymerase chain reaction (RT-qPCR). RNA was isolated from formalin-fixed paraffin-embedded (FFPE) tissue samples using the Maxwell 16 Instrument (Promega, Madison, WI, USA) with the Maxwell 16 LEV RNA FFPE kit (Promega). RT-qPCR analyses were performed using the GoTaq® Probe 2-step RT-qPCR System kit (Promega), according to the manufacturer's instructions. Reverse transcription was performed in a final volume of 20 μl containing 5 μl of RNA, as follows: 5 min at 25°C, 45 min at 42°C and 15 min at 70°C. Quantitative PCR was performed in a final volume of 20 μl containing 2 μl of cDNA with 0.2 μM primer for each gene, 0.1 μM of each DNA probe and GoTaq Probe real-time PCR Master Mix 2× (Promega) using this thermal profile: 2 min at 95°C and 50 cycles of 15 sec at 95°C and 1 min at 60°C for *YAP1::NUTM1* or 1 min at 55°C for *YAP1::MAML2*. *B2M* was used as reference gene. PCR reactions were performed on the LightCycler® 480 II (Roche, Indianapolis, IN, USA). For positive results in RT-qPCR, PCR products were purified by a mix of FastAP thermosensitive alkaline phosphatase and exonuclease I (Thermo-Fisher Scientific, Waltham, MA, USA) with the following conditions: 15 min at 37°C and 15 min at 85°C. The sequencing reaction was carried out using Big Dye terminator version 3.1 cycle sequencing kit (Applied Biosystems, Waltham, MA, USA) according to the manufacturer's protocol, and the subsequent steps: 1 min at 96°C followed by 30 cycles of 20 sec at 96°C, 15 sec at 50°C and 4 min at 60°C. Products were purified by the BigDye XTerminator™ purification kit (Applied Biosystems) as recommended and were sequenced on a Genetic Analyser (Applied Biosystems). The sequencing data were analysed using the sequencing analysis software (Applied Biosystems). Primers sequences are available in Supporting information, Method S2.

WHOLE-EXOME RNA-SEQUENCING

Whole-exome RNA-capture sequencing was performed as described previously.[18] In brief, total RNAs were extracted from FFPE tissue sections using a ForMaPure RNA kit (Beckman Coulter, Brea, CA, USA), and the Ambion DNase I (Life Technologies, Carlsbad, CA, USA) was used to remove DNA. RNA quantification was assessed using a NanoDrop spectrophotometer (ThermoFisher Scientific) measurement and RNA quality using the DV200 value (the proportion of the RNA fragments larger than 200 nt) assessed using a TapeStation with Hs RNA screen tape (Agilent, Santa

Clara, CA, USA). Samples with sufficient RNA quantity (>0.5 μg) and quality (DV200 > 30%) were considered suitable for sequencing. Individual libraries were prepared using 100 ng of total RNA and TruSeq RNA Exome kits (Illumina, San Diego, CA, USA). Twelve libraries were pooled at a concentration of 4 nM each, together with 1% PhiX spike as control. Sequencing was performed (paired end, 2×75 cycles) using NextSeq 500/550 high output kits on a NextSeq 500 machine, or the NovaSeq 6000 SP/S1 reagent kit on a NovaSeq 6000 machine (Illumina).

The mean number of reads per sample was approximately 80 million. Alignments were performed using STAR on the GRCh38 version of the human reference genome.[19] Numbers of duplicate reads were assessed using Picard tools (Broad Institute, Picard; available at: http://broadinstitute.github.io/picard). Samples with a number of unique reads under 10 million were discarded from further analyses. An average of ×130 depth of analysis was ensured using this technique. Fusion transcripts were typically called by six different algorithms, including STAR-Fusion (Broad Institute; STAR-Fusion: Fast and Accurate Fusion Transcript Detection from RNA-Seq;[20] available at: http://star-fusion.github.io), FusionMap,[21] Fusion-Catcher (FusionCatcher – a tool for finding somatic fusion genes in paired-end RNA-sequencing data),[22] TopHat-Fusion,[23] EricScript[24] and Arriba (Uhrig S. Arriba – fast and accurate gene fusion detection from RNA-Seq data 2019; available at: https://github.com/suhrig/arriba). Variant calling was performed using the GATK HaplotypeCaller (scaling accurate genetic variant discovery to tens of thousands of samples[25]), then filtering and annotation were achieved with the ANNOVAR annotation tool.[26] Expression values were extracted using the Kallisto version 0.41 tool with GENCODE release 23-genome annotation based on GRCh38 reference.[27,28] Kallisto TPM expression values were transformed in $\log_2$ (TPM + 2), and all samples were normalised together using the quantile method from the R limma package within R (version 3.1.1) environment (Linear Models for Microarray Data).[29]

DETECTION OF *RB1* PATHOLOGICAL VARIANTS AND DELETION

Genomic DNA was isolated using the Maxwell 16 FFPE Plus LEV DNA purification kit (Promega) and analysed on an Illumina NextSeq gene sequencer using the Breast cancer panel (Qiagen, Germantown, MD, USA), including *RB1*. Only pathological variants were selected on VarSome ('pathogenic' or 'probably pathogenic').

FISH ANALYSIS

FISH was performed on 4 μm sections of FFPE tissue using the ZytoLight SPEC RB1/13q12 and FISH-Tissue Implementation Kit (#Z-2028-20; Zytovision, Bremerhaven, Germany), as instructed.

MCPYV STATUS DETERMINATION

MCPyV status was determined in Merkel cell carcinoma cases using RT-PCR, as previously described.[16] The Merkel cell carcinoma cell line WaGa (RRID: CVCL_E998) was used as positive control.

CELL CULTURE AND LENTIVIRAL TRANSDUCTION

The HaCaT (RRID: CVCL_0038) was grown in DMEM supplemented with 10% FCS, 100 U/ml penicillin and 0.1 mg/ml streptomycin and amphotericin B. All cells were grown at 37°C, 5% CO_2 in a humidified incubator. Plasmid encoding large T antigen (pcdh-LT)[30] and shRNA targeting *RB1*[31] were used as previously described. Lentiviral infections were performed as previously described.[32] The selection of transduced cell was performed with puromycin at 2.5 μg/ml for pcdh-LT for 1 week.

IMMUNOBLOT

Immunoblotting was performed as previously described.[33] Antibodies used in this study were directed against Large T (clone CM2B4, 1:500), Rb (clone 1F8, 1/200), YAP1 (YAP1 (C-ter), clone D8H1X, 1:1000) and β-actin (clone A1978; Sigma, Lezennes, France; 1:1000).

STATISTICAL ANALYSES

Continuous data are described by medians and ranges and categorical data by percentage of interpretable cases. The local Ethics Committee in Human Research of Tours (France) approved the study (no. ID RCB2009-A01056-51).

Patient consent was obtained via a no-objection form, which was sent to all participants. The data sets used and/or analysed during the current study are available from the corresponding author upon reasonable request.

Results

LACK OF YAP1 EXPRESSION IS FREQUENT IN POROMA, POROCARCINOMA, *IN-SITU* AND INVASIVE POORLY DIFFERENTIATED SQUAMOUS CELL CARCINOMA AND MERKEL CELL CARCINOMA

To confirm previous results on C-ter YAP1 immunohistochemistry as a relevant diagnostic marker for poroid tumours, we evaluated its expression in a cohort of 511 cutaneous skin epithelial tumours embedded in TMA and 32 cases on whole-slides, including poroma ($n = 26$), poroid hidradenoma ($n = 1$), porocarcinoma ($n = 14$), invasive squamous cell carcinoma ($n = 58$), squamous cell carcinoma in situ ($n = 35$), basal cell carcinoma ($n = 47$), clonal seborrhoeic keratosis ($n = 1$), large cell acanthoma ($n = 5$), Merkel cell carcinoma ($n = 165$), trichoblastoma ($n = 19$), inverted follicular keratosis ($n = 1$), trichilemmoma ($n = 4$), trichoepithelioma ($n = 5$), proliferating pilar cyst ($n = 2$), sebaceoma ($n = 19$), sebaceous carcinoma ($n = 60$), sebaceous adenoma ($n = 51$), hidradenoma ($n = 6$), chondroid syringoma ($n = 3$), spiradenoma ($n = 11$), cylindroma ($n = 1$), Paget ($n = 5$), adnexal carcinoma, NOS ($n = 1$), adenoid cystic carcinoma ($n = 1$) and myoepithelioma ($n = 2$). Results are summarised in Table 1 and Figure 1.

Notably, among the SCC samples included in the cohort, 18 cases were initially referred to our centres with an initial diagnosis of porocarcinoma but were later reclassified as SCC: these cases have been studied on whole-slides. The characteristics of these morphological mimickers of porocarcinoma are available in Table 2 and Figure 2.

Among poroma and poroid hidradenoma, the loss of YAP1 was observed in 24 cases (89%), while its expression was preserved in three cases. Among the YAP1 non-expressing poroma with sufficient material for molecular investigation ($n = 21$), YAP1 fusion was demonstrated in 16 cases (76%), with 33 and 43% of fusion involving *MAML2* and *NUTM1*, respectively. All cases with a fusion of *NUTM1* exhibited diffuse nuclear staining of NUT (Figure 1). Importantly, YAP1 fusion transcript was not detected in five cases of immunohistochemically YAP1 non-expressing poroma by our PCR approach, and lack of sufficient material did not allow for further whole-exome RNA-sequencing in these cases.

In cases morphologically classified as porocarcinoma ($n = 14$), the complete loss of YAP1 expression was detected in 10 porocarcinoma cases (72%), all with confirmed YAP1 fusion of either *YAP1*::*MAML2* ($n = 6$, 43%) or *YAP1*::*NUTM1* ($n = 4$, 29%). Among

the 18 porocarcinoma mimickers, eight cases of *in-situ* and invasive SCC with bowenoid characteristics and all pseudoglandular SCC ($n = 3$) showed a preserved expression of YAP1 (53%). By contrast, complete loss of YAP1 was demonstrated in three cases (17%) of in-situ and invasive SCC with bowenoid characteristics, while its partial loss was observed in four cases (22%). However, fusion transcripts were never detected in this subgroup, confirming the detection of fusions as a relevant tool for the diagnosis of porocarcinoma (Table 2).

Among other tumours (Table 1), complete loss of YAP1 was observed in 11 additional cases (15%) of in-situ or invasive SCC (Figure 3A), in 162 cases (98%) of MCC (115 MCPyV(+) cases, 36 MCPyV(−) cases and 11 cases with unknown MCPyV status) (Figure 3B), in one case of trichoblastoma and one case of a tumour diagnosed as sebaceoma (Supporting information, Figure S1). Interestingly, applying molecular investigation to all YAP1 non-expressing cases of SCC, trichoblastoma, sebaceoma and 10 cases of MCC, no fusion transcript was detected except in the only case diagnosed as sebaceoma. Importantly, we detected in this case a non-canonical *YAP1*::*MAML2* fusion with insertion of an intron portion in the coding sequence (Supporting information, Figure S1). To evaluate whether the *YAP1* gene could be rearranged with other partners, eight cases of YAP1 non-expressing MCC (five MCPyV-positive and three MCPyV-negative cases) were submitted for whole-exome RNA capture-sequencing, which did not reveal any *YAP1* or other relevant fusion. (Supporting information, Table S1).

Therefore, our results suggest that while *YAP1* fusions are almost restricted to poroma and porocarcinoma among skin tumours, loss of YAP1 expression is observed in *YAP1* rearranged tumours, and also in Merkel cell carcinoma and in a subset of squamous cell carcinoma.

IN CONTRAST TO SCC WITH BOWENOID CHARACTERISTICS, POROCARCINOMA WITH *YAP1* FUSION SHOWS PRESERVED EXPRESSION OF RB

Reduced YAP1 expression due to transcriptional repression related to *RB1* inactivation has been reported in other organs.[10,11,34] In this context we aimed to determine whether YAP1 expression might be affected in a similar manner in skin tumours. In particular, the loss of YAP1 expression was detected in most of the MCC, which shows almost constant inactivation of Rb, either due to MCPyV oncoprotein expression or *RB1* mutation or deletion.[31,35,36]

Table 1. YAP1 immunohistochemical expression in skin epithelial tumours (study on TMA, $n = 511$ and whole-slide, $n = 32$ – total, $n = 543$)

Histological subtype	YAP1 expression	
	Absence	Presence
Poroid tumours ($n = 41$)		
Poroma ($n = 26$)	23 (88%)	3 (12%)
Poroid hidradenoma ($n = 1$)	1 (100%)	0
Porocarcinoma ($n = 14$)	10 (72%)	4 (28%)
Keratinocytic/epidermal tumours ($n = 311$)		
Invasive squamous cell carcinoma ($n = 58$)*	8 (14%)	50 (86%)
Squamous cell carcinoma *in situ* ($n = 35$)*	6 (18%)	29 (82%)
Basal cell carcinoma ($n = 47$)	0	47 (100%)
Clonal seborrhoeic keratosis ($n = 1$)	0	1 (100%)
Large cell acanthoma ($n = 5$)	0	5 (100%)
Merkel cell carcinoma ($n = 165$)	162 (98%)	3 (2%)
Tumours with follicular differentiation ($n = 31$)		
Trichoblastoma ($n = 19$)	1 (5%)	18 (95%)
Inverted follicular keratosis ($n = 1$)	0	1 (100%)
Trichilemmoma ($n = 4$)	0	4 (100%)
Trichoepithelioma ($n = 5$)	0	5 (100%)
Proliferating pilar cyst ($n = 2$)	0	2 (100%)
Tumour with sebaceous differentiation ($n = 130$)		
Sebaceoma ($n = 19$)	1 (5%)	18 (95%)
Sebaceous carcinoma ($n = 60$)	0	60 (100%)
Sebaceous adenoma ($n = 51$)	0	51 (100%)
Tumour with apocrine/eccrine differentiation ($n = 30$)		
Hidradenoma ($n = 6$)	0	6 (100%)
Chondroid syringoma ($n = 3$)	0	3 (100%)
Spiradenoma ($n = 11$)	0	11 (100%)
Cylindroma ($n = 1$)	0	1 (100%)
Paget ($n = 5$)	0	5 (100%)
Adnexal carcinoma, NOS ($n = 1$)	0	1 (100%)

Table 1. (*Continued*)

Histological subtype	YAP1 expression	
	Absence	Presence
Adenoid cystic carcinoma ($n = 1$)	0	1 (100%)
Myoepithelioma ($n = 2$)	0	2 (100%)

*Including the 18 'porocarcinoma mimickers' included in Table 2.

To confirm whether the inactivation of Rb induced the repression of YAP1 expression, shRNA-induced *RB1* knockdown and ectopic MCPyV Large T expression were achieved *in vitro* in immortalised keratinocytes (HaCat cells) using lentiviral vectors. These experiments resulted in a drastic reduction in the expression of YAP1 in *RB1* knockdown cells compared to controls (Figure 3C,D), suggesting that the Rb inactivation through the expression of Large T or genetic inactivation in Merkel cell carcinoma resulted in the repression of YAP1 expression.

Among non-MCC, YAP1 non-expressing tumours of the cohort, all but one case of YAP1 non-expressing SCC ($n = 14$) demonstrated complete loss of Rb expression by immunohistochemistry (Figure 3A), while all but one porocarcinoma case, including all cases with a fusion of *YAP1*, showed a preserved expression of Rb (Supporting information, Figure S2). Additionally, genetic investigation of four cases of YAP1 non-expressing Rb-deficient SCC revealed mutations and/or deletion of *RB1* (Supporting information, Table S2), confirming genetic inactivation of the *RB1* gene. Moreover, investigation of Rb expression in the group of mimickers of porocarcinoma revealed the complete loss of Rb in most cases ($n = 10$, 55%), including all tumours with reduced/absent expression of YAP1 (Table 2).

Together, these results support that Rb inactivation constituted a frequent alternative mechanism leading to the repression of YAP1 transcription in several skin tumour histotypes, including Merkel cell carcinoma, *RB1*-deficient in-situ and invasive SCC, but appeared somewhat exceptional in *YAP1*-rearranged porocarcinoma.

Therefore, our data strongly suggest that *RB1*-deficient in-situ or invasive SCC with bowenoid characteristics, which represents a differential diagnosis of porocarcinoma, can show a reduction or complete loss of YAP1 expression without a detectable *YAP1* gene fusion.
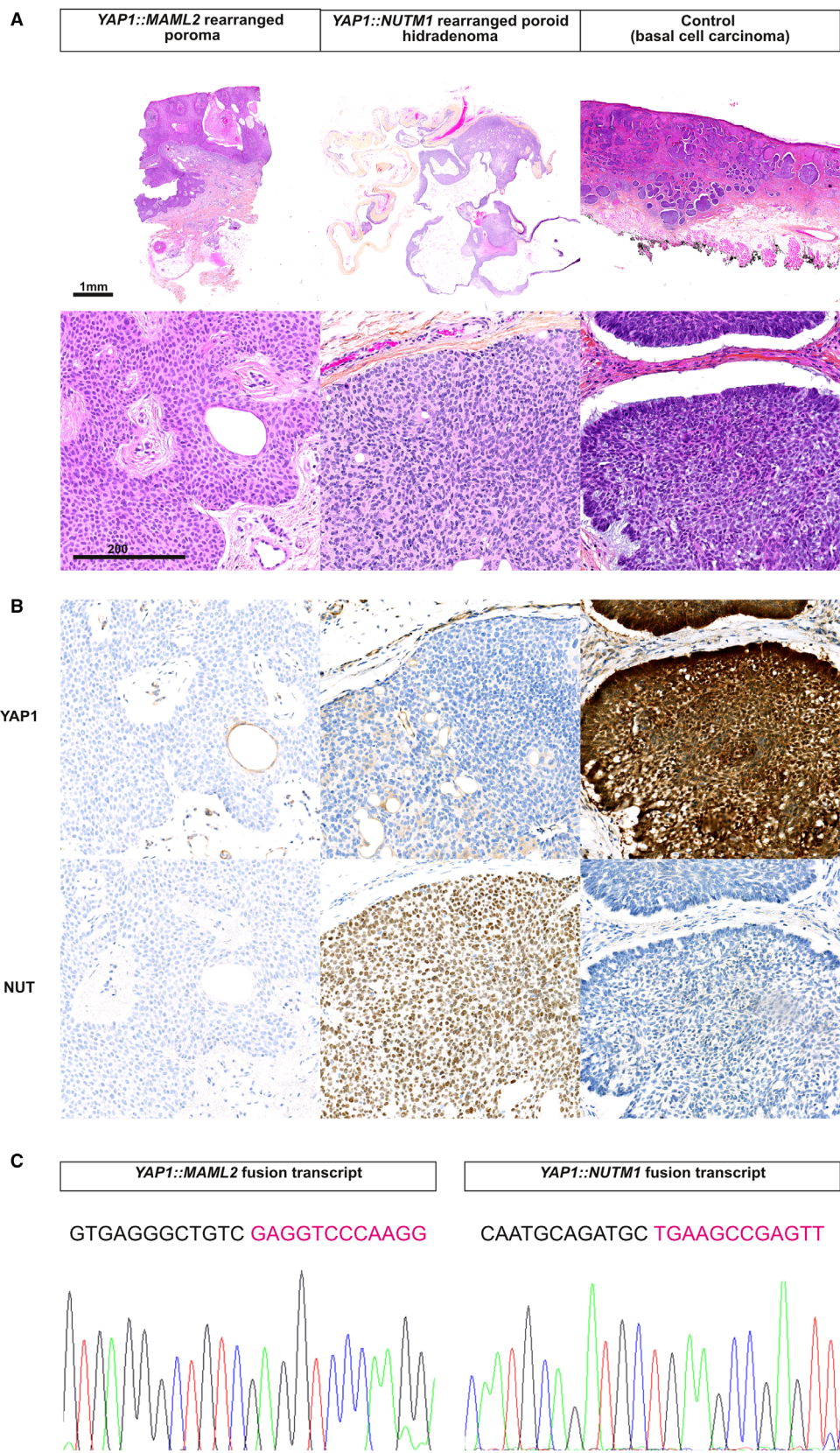
Figure 1. Detection of YAP1 expression and YAP1 gene rearrangements in poroma tumours and controls. A poroma, a poroid hidradenoma and an invasive basal cell carcinoma are depicted. A, Morphological features of the cases. Poroma and poroid hidradenoma differ by their silhouette but are both composed of round poroid monotonous cells, with oval nucleus, scant cytoplasm and ductal formations. Invasive basal cell carcinoma shows a different architecture, with clefting, nuclear palisading and a cellular fibromyxoid stroma. B, Immunohistochemical features of the cases. Both poroma and poroid hidradenoma neoplasms show complete loss of C-Ter YAP1 expression while the expression of this protein was preserved in basal cell carcinoma. In addition, the poroid hidradenoma also shows NUT expression. C, Molecular features of the cases. Sanger sequencing reveals *YAP1::MAML2* and *YAP1::NUTM1* fusion transcripts in poroma and in poroid hidradenoma, respectively.

Table 2. Clinical, histopathological and molecular features of porocarcinoma cases and mimickers (study on whole-slide, *n* = 32)

	Poro-carcinoma (*n* = 14)	Bowen disease (*n* = 8)	SCC with bowenoid characteristics (*n* = 7)	Pseudo-glandular SCC (*n* = 3)
Clinical features				
Age (years)				
Years (median = Q1–3)	73 (58–87)	79 (75–85)	97 (81–88)	79 (64–80)
Sex				
F/M	9/5	3/5	2/5	0/3
Size				
mm (median = Q1–3)	12 (9–16)	11 (9–13)	25 (19–28)	10 (7–25)
Sites				
Head and neck	0	0	2 (28%)	3 (100%)
Trunk	2 (14%)	1 (12%)	0	0
Upper limb	1 (7%)	2 (25%)	2 (28%)	0
Lower limb	11 (79%)	5 (63%)	3 (44%)	0
Microscopic features				
Infiltration				
In situ	1 (7%)	8 (100%)	0	0
Pushing	7 (50%)	0	5 (72%)	1 (33%)
Infiltrative	6 (43%)	0	2 (28%)	2 (67%)
Cytological atypia				
Mild	9 (64%)	1 (12%)	0	0
Severe	5 (36%)	7 (88%)	7 (100%)	3 (100%)
Mature duct formation	9 (64%)	0	0	0
Intracytoplasmic lumina/cell vacuolisation	9 (64%)	6 (75%)	6 (89%)	2 (67%)
Acantholysis	0	2 (25%)	0	3 (100%)
Pseudoglandular formation	0	0	0	3 (100%)
Benign component	9 (64%)	0	0	0
Bowen disease	0	8 (100%)	4 (57%)	0
Necrosis				
Comedonecrosis	6 (43%)	1 (12%)	5 (71%)	1 (33%)
Diffuse	1 (7%)	0	1 (14%)	0
Bowenoid pattern*	4 (28%)	0	7 (100%)	0
Clear cell change	9 (64%)	5 (63%)	5 (71%)	0
Squamous differentiation	0	1 (12%)	0	1 (33%)

Table 2. (*Continued*)

	Poro-carcinoma (*n* = 14)	Bowen disease (*n* = 8)	SCC with bowenoid characteristics (*n* = 7)	Pseudo-glandular SCC (*n* = 3)
Spindle cell change	3 (21%)	4 (50%)	2 (28%)	1 (33%)
Colonisation by melanocytes	1 (7%)	0	1 (14%)	0
Immunohistochemical profile				
CEA**				
Tumour ducts	9 (64%)	0	0	0
Rb				
Preserved	5 (39%	2 (28%)	1 (14%)	3 (100%)
Partial loss***	7 (53%)	1 (14%)	0	0
Complete loss***	1 (8%)	4 (58%)	6 (86%)	0
Unavailable data	1	1	0	0
C-Ter YAP1				
Preserved	3 (21%)	5 (64%)	3 (44%)	3 (100%)
Partial loss	1 (7%)	2 (24%)	2 (28%)	0
Complete loss	10 (72%)	1 (12%)	2 (28%)	0
Unavailable data	0	0	0	0
Molecular features				
YAP1::MAML2	6 (43%)	0	0	0
YAP1::NUTM1	4 (29%)	0	0	0

*The bowenoid pattern was defined as previously described:[3] 'A variant of invasive tumour having a broad pushing advancing edge with focal dyskeratosis and often-bizarre cytonuclear atypia reminiscent of Bowen's disease [squamous carcinoma (SCC) *in situ*]'.
**The detection of tumour duct in porocarcinoma was further confirmed using at least one of the following markers: CK7, CK19 or EMA.
***The partial and complete loss of Rb expression were evaluated as previously described,[15] with only complete loss associated with RB1 mutation.[15]

Discussion

Since gene fusions have been demonstrated in poroma and porocarcinoma,[7] YAP1 immunohistochemistry has been suggested to be a relevant surrogate to molecular testing. In the present study, we further confirmed these findings by analysing its specificity in a large set of skin neoplasms. Interestingly, in addition to poroma and porocarcinoma cases, the absence of expression of YAP1 was also observed in a subset of SCCs showing *RB1*-inactivation as well as in almost all cases of MCC tested, while all these cases lacked detectable fusion of *YAP1* by molecular testing, suggesting other mechanisms involved in the repression of YAP1.

Previous *in-vitro* experiments strongly suggested that YAP1 expression was repressed in the setting of *RB1*-inactivation, which is a hallmark of high-grade neuroendocrine tumours, including MCC. Consequently, we have demonstrated the reduction or extinction of YAP1 in other subtypes of *RB1*-deficient cutaneous carcinomas and further confirmed *in vitro* that the inactivation of Rb, through ARN interference or Large T sequestration, resulted in a reduction in YAP1 expression. In line with these results, the expression of YAP1 was evaluated on whole-slides in porocarcinoma and morphological mimickers, including Bowen disease, poorly differentiated invasive SCC with bowenoid characteristics and pseudoglandular SCC. Although rearrangements of *YAP1* were
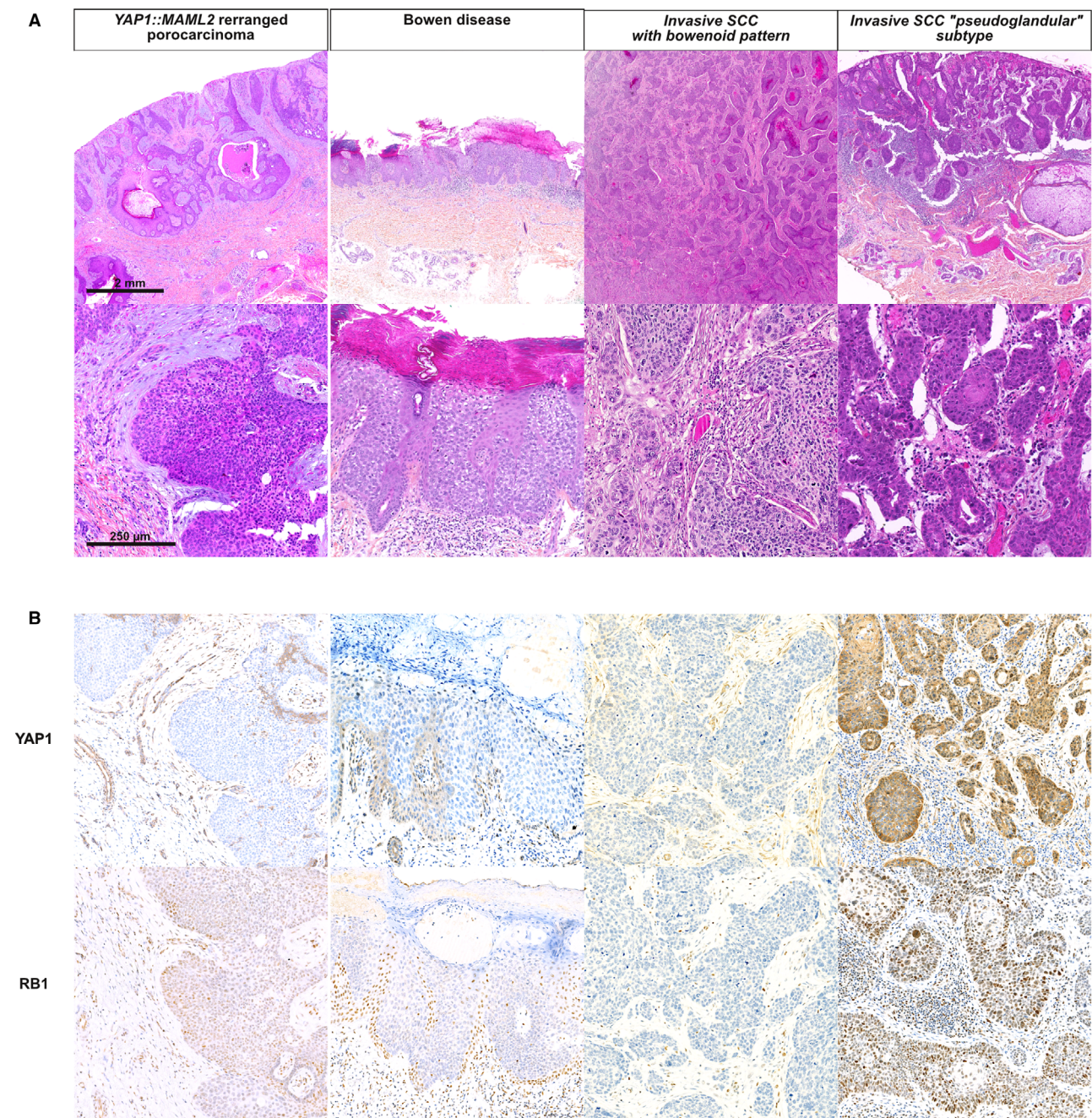
Figure 2. Morphological and immunohistochemical features of porocarcinoma and mimickers. A porocarcinoma and three variants of squamous cell carcinoma are depicted. A, Morphological features of the cases. B, Detection of YAP1 and Rb by immunohistochemistry. Porocarcinoma consists of a malignant proliferation of tumour cells forming ducts with connection to the epidermis and lack of YAP1 and Rb expression. Bowen disease and invasive SCC with bowenoid characteristics are composed of poorly differentiated, atypical cells, devoid of keratinisation but with frequent comedonecrosis. Both of the latter show lack of YAP1 and Rb expression. To note, a preserved basal layer of keratinocytes showing YAP1 expression is frequently observed in poroma. Acantholytic (pseudovascular) squamous cell carcinoma is a mimicker of porocarcinoma owing to its morphology, with often formation of pseudoglandular or pseudovascular spaces. However, this example of SCC lacks bowenoid characteristics and shows preserved YAP1 and RB1 expression.

exclusively detected in cases of porocarcinoma a lack of expression of YAP1 was observed in porocarcinoma and SCC, while inactivation of *RB1* was

detected in most bowenoid SCCs (66%). These data suggest that *in-situ* or invasive poorly differentiated *RB1*-deficient SCC with bowenoid characteristics can
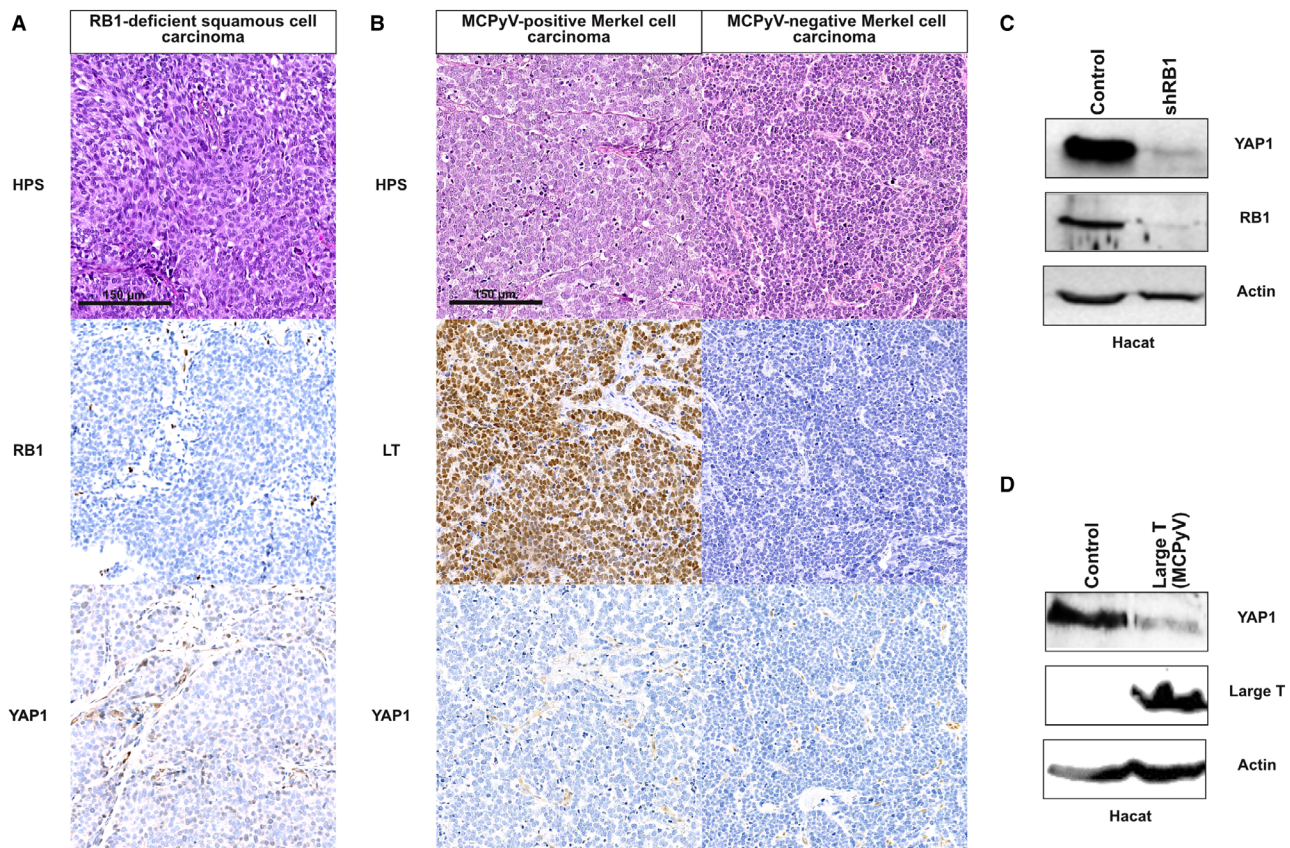
Figure 3. Expression of YAP1 in RB1-deficient carcinoma. A, Investigation of expression of Rb and C-Ter YAP1 expressions in RB1-deficient squamous cell carcinoma with bowenoid characteristics. Morphologically the cells show poor differentiation, no keratinisation, nuclear atypia, mitotic figures and occasional necrotic cells. Immunohistochemical investigation evidences a complete lack of RB1 and YAP1 expression in this case. B, Investigation of C-Ter YAP1 expression in Merkel cell carcinoma. An MCPyV-positive and an MCPyV-negative case is depicted, with respective expression or lack of expression of the viral oncoprotein Large T. Both cases show constant lack of YAP1 expression. C,D, Detection of YAP1 expression by Western blot in HaCat cells transduced with an empty vector (controls) or after transduction of shRNA targeting RB1 (C) or ectopic expression of the Large T (D). Reduced YAP1 expression was observed after Rb inactivation either due to reduced expression (shRNA) or due to Large T antigen expression. [Colour figure can be viewed at wileyonlinelibrary.com]

demonstrate reduced or absent expression of YAP1. Due to their frequent loss of YAP1 expression and overlapping morphological characteristics, this subset of SCC constitutes a diagnostic pitfall with porocarcinoma. Therefore, molecular testing or combined immunohistochemical detection of Rb and YAP1 may be required to clearly distinguish *YAP1*-rearranged porocarcinoma from *RB1*-deficient YAP1 non-expressing poorly differentiated carcinoma, including Bowen disease.

SCC is considered the main differential diagnosis of porocarcinoma,[3,37] in particular Bowen disease and invasive SCC with bowenoid characteristics, both showing characteristics overlapping with porocarcinoma such as high-grade cytology, poorly differentiated basophilic morphology ('bowenoid pattern'), frequent comedonecrosis and lack of keratinisation.

By investigating a series of 31 cases diagnosed as poroma and porocarcinoma without investigating the fusion of *YAP1*, Harms *et al.* have observed diffuse or focal loss of Rb expression as well as aberrant p53 staining almost restricted to the porocarcinoma group, and concluded that inactivation of *TP53* and *RB1* could contribute to transformation.[15] Importantly, in this study the diffuse aberrancy in p53 and Rb expression correlated with tumour mutations in *TP53* and *RB1*, respectively, whereas focal Rb loss was associated with wild-type *RB1*.[15] Also importantly, data from other studies have reported that inactivating *RB1* mutations were restricted to a minority (approximately 10%) of cutaneous SCC[13,38,39] which were likely to show a distinctive morphology and expression profiles[13,40,41] compared to wild-type *RB1* cases. In our study, complete loss of

Rb expression was never observed in *YAP1*-rearranged porocarcinoma, but was frequent in Bowen disease and highly prevalent in SCC with bowenoid characteristics, which showed frequent *RB1* mutations and/or deletion.

In other solid cancers, inactivation of *RB1*, resulting in E2F release, induces transcriptional repression of the *YAP1* gene.[11,34,42] Although *YAP1* acts as an oncogene in most solid tumours, its inactivation contributes to the progression of *RB1*-deficient cancers, including retinoblastoma and small cell carcinoma of the lung.[34] Merkel cell carcinoma is a rare skin neuroendocrine carcinoma induced by integration of Merkel cell polyomavirus in approximately 80% of cases,[12] while 20% of the remaining tumours are related to UV-induced DNA damage.[43] Importantly, inactivation of Rb through protein sequestration by viral oncoprotein or following a genetic alteration (mutation/deletion)[43] is a crucial mechanism for the development of MCC. In contrast to the initial report by Sekine *et al.*,[7] we observed a lack of YAP1 expression in almost all Merkel cell carcinomas in the present study, suggesting that inactivation of YAP1 could be a necessary event for the development of MCC, as observed for neuroendocrine carcinomas; notably, small cell carcinoma of the lung.[34]

Furthermore, *RB1*-deficient SCC was recently identified as potential a precursor of MCPyV-negative tumours.[38,40,41] In fact, up to 50% of MCPyV-negative cases are associated with an SCC component, and genetic analysis recently demonstrated the clonal link between the two tumours.[38,40,41] Furthermore, inactivation of *RB1* through mutation or deletion is constantly observed in both components of these tumours, suggesting that inactivation of *RB1* is a necessary preliminary step for the development of MCPyV-negative tumours. It is not yet clear how *RB1* inactivation contributes to the acquisition of the neuroendocrine phenotype. However, YAP1 expression is inversely correlated with INSM1 and other neuroendocrine markers in models of small cell lung cancer, suggesting that *YAP1* repression is related to acquisition of the neuroendocrine phenotype.[11]

Similarly, it might be possible that, in combined tumours, *YAP1* repression through *RB1* inactivation in the SCC component could contribute to its transformation into MCC in the skin. Interestingly, while investigating a series of 15 combined MCC, Martin *et al.* identified one case that harboured an MCC and a porocarcinoma-like component.[44] Consequently, we recently observed a similar case (personal observation) that harboured loss of Rb and YAP1 expression by immunohistochemistry without *YAP1::MAML2*

fusion. These findings further support the fact that *RB1*-deficient SCC and porocarcinoma are morphologically close and can both exhibit loss of YAP1 expression.

In their initial report, Sekine *et al.* suggested a combined use of two antibodies targeting both extremities of the YAP1 protein could distinguish fusion from transcriptional repression. However, using the same method we observed a combined loss of both extremities of YAP1 in rearranged poroma cases (Supporting information, Figure S3 and Table S3). Therefore, our results suggest that the combined use of Rb and YAP1 C-Ter immunohistochemistry may be more relevant than C- and N-terminal YAP1 targeting antibodies for the differential diagnosis between porocarcinoma and poorly differentiated *RB1*-inactivated SCC.

In conclusion, in the present study we have confirmed the loss of YAP1 expression that reflects rearrangement of *YAP1* in most cases of poroma and porocarcinoma. Furthermore, we demonstrated repression of YAP1 expression in cutaneous carcinoma with Rb-inactivation, including MCC and a subset of SCC, the latter being the main differential diagnosis of porocarcinoma in current practice.

Acknowledgements

Conflicts of interest

All authors have no conflicts of interest to disclose.

References

1. WHO. WHO classification of skin tumours. 4th edition. In Elder DE, Massi D, Scolyer RA, Willemze R eds. *Lyon: international agency for research on cancer*. Lyon, France: World Health Organization classification of tumours, 2018; 470.

2. Behbahani S, Malerba S, Karanfilian KM, Warren CJ, Alhatem A, Samie FH. Demographics and outcomes of eccrine porocarcinoma: results from the National Cancer Database. *Br. J. Dermatol.* 2020; **183**; 161–163.

3. Robson A, Greene J, Ansari N *et al.* Eccrine porocarcinoma (malignant eccrine poroma): a clinicopathologic study of 69 cases. *Am. J. Surg. Pathol.* 2001; **25**; 710–720.

4. Snow SN, Reizner GT. Eccrine porocarcinoma of the face. *J. Am. Acad. Dermatol.* 1992; **27**(2 Pt 2); 306–311.

5. Kottler D, Rivet J, Hickman G. Porocarcinome eccrine bowénoïde: un carcinome annexiel de diagnostic difficile. *Ann. Pathol.* 2014; **34**; 378–383.

6. Obi M, Satoh T, Yokozeki H, Nishioka K. Eccrine porocarcinoma with Bowenoid changes: epithelial membrane antigen is not a useful marker for malignant tumours arising from

eccrine gland structures. *Acta Derm. Venereol.* 2004; **84**; 142–144.

7. Sekine S, Kiyono T, Ryo E *et al.* Recurrent YAP1-MAML2 and YAP1-NUTM1 fusions in poroma and porocarcinoma. *J. Clin. Invest.* 2019; **129**; 3827–3832.

8. Russell-Goldman E, Hornick JL, Hanna J. Utility of YAP1 and NUT immunohistochemistry in the diagnosis of porocarcinoma. *J. Cutan. Pathol.* 2021; **48**; 403–410.

9. Anderson WJ, Fletcher CDM, Hornick JL. Loss of expression of YAP1 C-terminus as an ancillary marker for epithelioid hemangioendothelioma variant with YAP1-TFE3 fusion and other YAP1-related vascular neoplasms. *Mod. Pathol.* 2021; **34**; 2036–2042.

10. Ito T, Matsubara D, Tanaka I *et al.* Loss of *YAP 1* defines neuroendocrine differentiation of lung tumors. *Cancer Sci.* 2016; **107**; 1527–1538.

11. McColl K, Wildey G, Sakre N *et al.* Reciprocal expression of INSM1 and YAP1 defines subgroups in small cell lung cancer. *Oncotarget* 2017; **8**; 73745–73756.

12. Feng H, Shuda M, Chang Y, Moore PS. Clonal integration of a polyomavirus in human Merkel cell carcinoma. *Science* 2008; **319**; 1096–1100.

13. Lazo de la Vega L, Bick N, Hu K *et al.* Invasive squamous cell carcinomas and precursor lesions on UV-exposed epithelia demonstrate concordant genomic complexity in driver genes. *Mod. Pathol.* 2020; **33**; 2280–2294.

14. Tetzlaff MT, Singh RR, Seviour EG *et al.* Next-generation sequencing identifies high frequency of mutations in potentially clinically actionable genes in sebaceous carcinoma. *J Pathol.* 2016; **240**; 84–95.

15. Zahn J, Chan MP, Wang G *et al.* Altered Rb, p16, and p53 expression is specific for porocarcinoma relative to poroma. *J Cutan Pathol.* 2019; **46**; 659–664.

16. Kervarrec T, Tallet A, Miquelestorena-Standley E *et al.* Diagnostic accuracy of a panel of immunohistochemical and molecular markers to distinguish Merkel cell carcinoma from other neuroendocrine carcinomas. *Mod Pathol.* 2019; **32**; 499–510.

17. Macagno N, Kervarrec T, Sohier P *et al.* NUT is a specific immunohistochemical marker for the diagnosis of YAP1-NUTM1-rearranged cutaneous poroid neoplasms. *Am. J. Surg. Pathol.* 2021; **45**; 1221–1227.

18. Cellier L, Perron E, Pissaloux D *et al.* Cutaneous Melanocytoma with CRTC1-TRIM11 fusion: report of 5 cases resembling clear cell sarcoma. *Am J Surg Pathol. mars* 2018; **42**; 382–391.

19. Dobin A, Davis CA, Schlesinger F *et al.* STAR: ultrafast universal RNA-seq aligner. *Bioinformatics* 2013; **29**; 15–21.

20. Haas BJ, Dobin A, Stransky N *et al.* STAR-fusion: fast and accurate fusion transcript detection from RNA-Seq. *Bioinformatics* 2017. https://doi.org/10.1101/120295.

21. Ge H, Liu K, Juan T, Fang F, Newman M, Hoeck W. FusionMap: detecting fusion genes from next-generation sequencing data at base-pair resolution. *Bioinformatics* 2011; **27**; 1922–1928.

22. Nicorici D, Satalan M, Edgren H *et al.* FusionCatcher - a tool for finding somatic fusion genes in paired-end RNA-sequencing data [internet]. *Bioinformatics* 2014. https://doi.org/10.1101/011650.

23. Kim D, Salzberg SL. TopHat-fusion: an algorithm for discovery of novel fusion transcripts. *Genome Biol.* 2011; **12**; R72.

24. Benelli M, Pescucci C, Marseglia G, Severgnini M, Torricelli F, Magi A. Discovering chimeric transcripts in paired-end RNA-seq data by using EricScript. *Bioinformatics* 2012; **28**; 3232–3239.

25. Poplin R, Ruano-Rubio V, DePristo MA *et al.* Scaling accurate genetic variant discovery to tens of thousands of samples [internet]. *Genomics* 2017. https://doi.org/10.1101/201178.

26. Wang K, Li M, Hakonarson H. ANNOVAR: functional annotation of genetic variants from high-throughput sequencing data. *Nucleic Acids Res.* 2010; **38**; e164.

27. Bray NL, Pimentel H, Melsted P, Pachter L. Near-optimal probabilistic RNA-seq quantification. *Nat Biotechnol.* 2016; **34**; 525–527.

28. Harrow J, Frankish A, Gonzalez JM *et al.* GENCODE: the reference human genome annotation for the ENCODE project. *Genome Res.* 2012; **22**; 1760–1774.

29. Smyth G, Hu Y, Ritchie M *et al.* limma [Internet]. Bioconductor; 2017 [cité 14 janv 2022]. Disponible sur: https://bioconductor.org/packages/limma

30. Houben R, Angermeyer S, Haferkamp S *et al.* Characterization of functional domains in the Merkel cell polyoma virus large T antigen. *Int. J. Cancer* 2015; **136**; E290–E300.

31. Hesbacher S, Pfitzer L, Wiedorfer K *et al.* RB1 is the crucial target of the Merkel cell polyomavirus large T antigen in Merkel cell carcinoma cells. *Oncotarget* 2016; **7**; 32956–32968.

32. Houben R, Adam C, Baeurle A *et al.* An intact retinoblastoma protein-binding site in Merkel cell polyomavirus large T antigen is required for promoting growth of Merkel cell carcinoma cells. *Int. J. Cancer* 2012; **130**; 847–856.

33. Kervarrec T, Samimi M, Hesbacher S *et al.* Merkel cell polyomavirus T antigens induce Merkel cell-like differentiation in GLI1-expressing epithelial cells. *Cancers (Basel)* 2020; **12**(7); 1989. https://www.ncbi.nlm.nih.gov/pmc/articles/PMC7409360/.

34. Pearson JD, Huang K, Pacal M *et al.* Binary pan-cancer classes with distinct vulnerabilities defined by pro- or anticancer YAP/TEAD activity. *Cancer Cell.* 2021; **39**; 1115–1134.e12.

35. Carter MD, Gaston D, Huang WY *et al.* Genetic profiles of different subsets of Merkel cell carcinoma show links between combined and pure MCPyV-negative tumors. *Hum. Pathol.* 2018; **71**; 117–125.

36. Starrett GJ, Thakuria M, Chen T *et al.* Clinical and molecular characterization of virus-positive and virus-negative Merkel cell carcinoma. *Genome Med.* 2020; **12**; 30.

37. Cardoso JC, Calonje E. Malignant sweat gland tumours: an update. *Histopathology* 2015; **67**; 589–606.

38. Kervarrec T, Appenzeller S, Samimi M *et al.* Merkel cell polyomavirus-negative-Merkel cell carcinoma originating from in situ squamous cell carcinoma: a keratinocytic tumor with neuroendocrine differentiation. *J. Invest. Dermatol.* 2022; **142** (3 Pt A); 516–527.

39. Pickering CR, Zhou JH, Lee JJ *et al.* Mutational landscape of aggressive cutaneous squamous cell carcinoma. *Clin. Cancer Res.* 2014; **20**; 6582–6592.

40. Harms PW, Verhaegen ME, Hu K *et al.* Genomic evidence suggests that cutaneous neuroendocrine carcinomas can arise from squamous dysplastic precursors. *Mod. Pathol.* 2021; **30**; 506–514.

41. DeCoste RC, Walsh NM, Gaston D *et al.* RB1-deficient squamous cell carcinoma: the proposed source of combined Merkel cell carcinoma. *Mod. Pathol.* 2022; **8**; 1829–1836.

42. Cheng L, Zhou Z, Flesken-Nikitin A *et al.* Rb inactivation accelerates neoplastic growth and substitutes for recurrent amplification of cIAP1, cIAP2 and Yap1 in sporadic mammary carcinoma associated with p53 deficiency. *Oncogene* 2010; **29**; 5700–5711.

43. Harms PW, Vats P, Verhaegen ME *et al.* The distinctive mutational spectra of polyomavirus-negative Merkel cell carcinoma. *Cancer Res.* 2015; **75**; 3720–3727.

44. Martin B, Poblet E, Rios JJ *et al.* Merkel cell carcinoma with divergent differentiation: histopathological and immunohistochemical study of 15 cases with PCR analysis for Merkel cell polyomavirus. *Histopathology* 2013; **62**; 711–722.

Supporting Information

Additional Supporting Information may be found in the online version of this article:

Table S1. Whole-Exome RNA-sequencing analysis of 8 cases of MCC.

Table 2. Characterization of genetic alteration of *RB1* gene in poorly differentiated SCC with Bowenoid characteristics.

Table 3. Investigation of YAP1 expression using N-terminal and C-terminal YAP1 targeting antibodies in a part of the cohort.

Method S1. Antibodies and dilution.

Method S2. Primer sequences for PCR.

Figure 1. Histopathological and immunohistochemical characteristics of cases of sebaceoma and trichoblastoma showing loss of YAP1 expression.

Figure 2. Histopathological characteristics of a case diagnosed as intraepidermal porocarcinoma, lacking fusion of *YAP1*.

Figure 3. Immunohistochemical detection of of YAP1 in a case of poroma, using antibodies that target the C-ter and N-ter portions of YAP1 protein.